Eur. Phys. J. A **11**, 421–426 (2001)

THE EUROPEAN PHYSICAL JOURNAL A

Lyapunov exponent, generalized entropies and fractal dimensions of hot drops

C.O. Dorso[1,2] and A. Bonasera[1,a]

[1] Laboratorio Nazionale del Sud, Istituto Nazionale di Fisica Nucleare, via S. Sofia 44, I-95123 Catania, Italy
[2] Departamento de Fisica, Facultad de Ciencias Exactas y Naturales Universidad de Buenos Aires Pabellon I, Ciudad Universitaria, Nuñez 1428 Buenos Aires, Argentina

Received: 16 March 2001 / Revised version: 15 May 2001
Communicated by P. Schuck

Abstract. We calculate the maximal Lyapunov exponent, the generalized entropies, the asymptotic distance between nearby trajectories and the fractal dimensions for a finite two-dimensional system at different initial excitation energies. We show that these quantities have a maximum at about the same excitation energy. The presence of this maximum indicates the transition from a chaotic regime to a more regular one. In the chaotic regime the system is composed mainly of a liquid drop while the regular one corresponds to almost freely flowing particles and small clusters. At the transitional excitation energy the fractal dimensions are similar to those estimated from the Fisher model for a liquid-gas phase transition at the critical point.

PACS. 25.70.Mn Projectile and target fragmentation – 05.45.-a Nonlinear dynamics and nonlinear dynamical systems – 05.70.Jk Critical point phenomena

Introduction

Infinite systems composed of particles interacting with a potential which displays short-range repulsion plus longer-range attraction have an Equation Of State (EOS) resembling the Van der Waals one [1], which exhibits phase transitions from solid to liquid, liquid to gas, etc. The features of the EOS of such a system are quite independent of the specific form of the two-body potential, *i.e.* a sum of Yukawa's or Lennard-Jones potential etc. A problem arises when the system is constituted of a finite number of particles N and it is not confined in a box. In such a limit, it is not strictly correct to define a critical point, on the other hand, it becomes very interesting to analyze how the system behaves as a function of its excitation energy. Intuitively, we expect that at low excitation energies a transition, from solid-like state to liquid-like state, for a finite system should be very similar to the infinite case limit [2]. This is so because at these low energies the attractive part of the potential is dominant and the system remains confined in a given, self-sustained volume. One of the most important magnitudes that one can study is the caloric curve, *i.e.*, the functional relationship between the temperature of the system and the excitation energy. If a finite system is ananlyzed in the frame of the canonical ensemble, the caloric curve displays the standard "rise-plateau-rise" pattern. On the other hand, in the frame of the microcanonical ensemble a backbending is displayed and thus a negative specific heat can be found [3–6]. At higher excitation energies the system is unable to remain confined and undergoes a fragmentation process. This kind of process is characterized by the appearance of a new degree of freedom, the one associated with the collective expansion. In this case, it has been found that many features of a thermodynamical liquid-gas transition are reproduced even if the system is as small as being formed by just 100 particles [5,6]. These features are mainly deduced from the analysis of asymptotic mass distributions and in particular one finds a power law in the mass yield for a given initial excitation energy. There have been also estimates of the critical exponents from data in nucleus-nucleus and cluster-cluster collisions [7,8]. On the other hand, the corresponding caloric curve does not show the usual increase in the temperature of the so-called "vapor branch" with the increase of the excitation energy, but instead a plateau is reached as the system enters the fragmentation regime [6,9]. In this case, the above-mentioned backbending is found, which results in a negative specific heat [10,11]. The Maximal Lyapunov Exponent (MLE) has been studied in Classical Molecular Dynamics (CMD) for a 3-dimensional system composed of 100 particles and for different initial excitation energies. In [12] a maximum in the MLE was found for an initial ex-

[a] e-mail: bonasera@lns.infn.it

citation energy where a power law in the mass yield, intermittency signal, largest variance in the size of the biggest fragment [5,13,14] are also obtained. It is the purpose of this work to strengthen and better characterize this result by analyzing the behavior of other important indicators of chaoticity, *i.e.* the asymptotic distance between trajectories [15,16], the Generalized Renyi's Entropies (GRE) and the generalized fractal dimensions [17].

In sect. 1 we describe the model we used to perform our numerical simulations. In sect. 2 we recall previous results regarding the properties of the caloric curve of isotropically excited disks that undergo fragmentation, we take advantage of this results to emphasize the role played by the collective expansion. In sect. 3 we focus on what we call the Global Maximum Lyapunov exponent and the asymptotic maximal distance d_∞ . In particular, we focus on the competition between the collective expansion (ordered motion) and inter-particle collisions (chaotic motion). In sect. 4 we analyze the behavior of the generalized entropies and fractal dimensions as a function of the excitation energy of the fragmenting system. Finally, we draw conclusions.

1 The model

As stated in the Introduction, we study the fragmentation of two-dimensional excited Lennard-Jones disks. The two-body interaction potential is taken as the truncated Lennard-Jones (6-12) potential:

$$V(r) = 4\epsilon \left[\left(\frac{\sigma}{r}\right)^{12} - \left(\frac{\sigma}{r}\right)^{6} - \left(\frac{\sigma}{r_{\rm c}}\right)^{12} + \left(\frac{\sigma}{r_{\rm c}}\right)^{6} \right] . \quad (1)$$

We took the cut-off radius as $r_{\rm c} = 3\sigma$. Energy and distance are measured in units of the potential well (ϵ) and the distance at which the potential changes sign (σ), respectively. The unit of time used is: $t_0 = \sqrt{\sigma^2 m/48\epsilon}$. We used the well-known Verlet algorithm (which conserves volumes in phase space) to integrate the classical equations of motion [18] taking $t_{\rm int} = 0.001 t_0$ as the integration time step. This led to energy being conserved approximately as one part per million.

We performed explosions of $N = 100$ particles, two-dimensional disks. The initial configurations are constructed by cutting a circular disk from a thermalized, periodic, Lennard-Jones system with $N = 256$ particles in each periodic cell. The degree of excitation can be easily controlled in this way by varying the density and temperature of the periodic system. The initial states of our disks are macroscopically characterized by their energy and density (taken as that of the periodic system). We studied a broad energy range which encompasses very different behaviors regarding the fragmentation pattern. In fact, the resulting asymptotic mass spectra go from "U" shaped, for low excitation energies, to exponentially decaying, for the higher excitation energies. In between these two extremes a power-law–like spectra can be detected.

2 The caloric curve of finite systems

We define the caloric curve of finite systems as the functional relationship between the temperature at which the system fragments and its excitation energy. This problem involves the determination of the time at which the system fragments and the calculation of the corresponding temperatures at this time. Such a calculation has been undertaken in ref. [9] and here we briefly summarize the methods used and quote the main results.

The determination of the time of fragment formation is related to our ability to detect fragments for a given set of numerical simulations of fragmenting events. In a series of papers one of us has undertaken the analysis of different algorithms and developed what has been dubbed as the Early Cluster Formation Model (ECFM). Following [19], clusters are defined as the Most Bound Partition (MBP) of the system, *i.e.* the set of clusters $\{C_i\}$ for which the sum of the fragment internal energies attains its minimum value. Then the magnitude that is to be minimized is

$$E_{\rm int}^{C_i} = \sum_i \left[\sum_{j \in C_i} K_j^{\rm c.m.} + \sum_{\substack{j,k \in C_i \\ j \le k}} V_{jk} \right] , \quad (2)$$

where the first sum in (2) is over the elements of the partition $\{C_i\}$, $K_j^{\rm c.m.}$ is the kinetic energy of particle j measured in the center-of-mass frame of the cluster which contains particle j, and V_{jk} stands for the inter-particle potential of particles j and k, both beloging to the cluster under consideration. As it can be seen, the calculation is a highly self-consistent one. On the one hand, the potential energy term in eq. (2) favors the presence of large and compact clusters, taking advantage of spatial correlations. On the other hand, the kinetic term is responsible for the appearance of clusters with a certain degree of correlations in momentum space. MBP clusters, being built as a result of this trade-off, are related with what is known as the most bound density fluctuation in phase space [19].

The algorithm developed to find the MBP is known as "Early Cluster Recognition Algorithm" (ECRA), it allowed to discover that highly excited drops fragment very early in the evolution, that this fragmentation takes place in phase space and that the fragments are formed before they can be recognized in configuration space. This approach has been used in many other studies of fragmentation dynamics [9,19–21]. ECRA searches for most bound density fluctuations in coordinate and momentum space, thus some valuable information about the system coordinate and velocity correlations at all times, specially at the very early stages of the evolution, can be extracted.

Once the fragments are detected at all times using the above-mentioned fragment recognition algorithms, one has to detect the time at which the fragmentation process is over. We call this time, the time of fragment formation $\tau_{\rm ff}$. We define it as that time at which the system has already broken up in pieces of different sizes and after which the resulting fragments only undergo simple evaporation processes, *i.e.* the fragments might evaporate a few

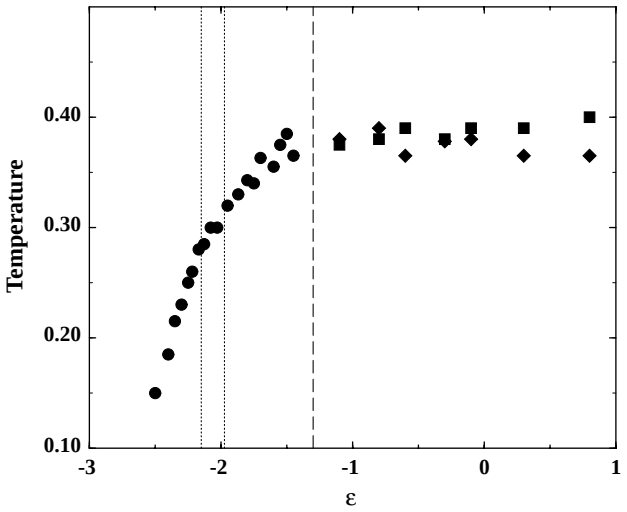

Fig. 1. Caloric curve for 2D Lennard-Jones disks. The transition from solid-like to liquid-like takes place in the region delimited by vertical dotted lines. The fragmentation region is to the right of the dashed vertical line. Full circles denote results from equilibrium calculations. Full squares denote the temperature of the fragmenting system at fragmentation time. Full diamonds stand for the mean temperature of fragments with mass bigger than 14 at asymptotic times.

monomers. For the estimation of $\tau_{\rm ff}$, it is then important to quantitatively measure the degree of similitude between any two given partitions belonging to the same evolution and corresponding to different times. We use the microscopic persistence coefficient P [9] to perform that task.

Given $X \equiv \{C_i\}$ and $Y \equiv \{C'_i\}$, two different partitions, we define:

$$P[X,Y] = \frac{1}{\sum_{\rm cl} n_i} \sum_{\rm cl} n_i \frac{a_i}{b_i}\,, \tag{3}$$

where b_i is the number of pairs of particles in the cluster C_i of partition X, a_i is the number of pairs of particles that belong to cluster C_i and also are together in a given cluster C'_j of partition Y, n_i is the number of particles in cluster C_i. The persistence coefficient is equal to one if the microscopic composition of the partition X equals the one of partition Y. On the other hand, it tends to zero when none of the constituent particles of a given cluster in X appear together in any given cluster in Y. From this, we determine the time of fragment formation $\tau_{\rm ff}$. Defining the caloric curve as the temperature of the system at the time of fragment formation $\tau_{\rm ff}$, dividing the system in concentric rings around the c.m. and calculating the temperature from the fluctuations of the velocity of the particles around the mean velocity of expansion of the above-mentioned rings, we get the caloric curve depicted in fig. 1 (for details of this calculation we refer to [9]). It is clear that the resulting caloric curve displays a simple rise plateau shape which lacks the usual vapor branch. This behavior has been traced to the role played by the collective mode of expansion that behaves as a heat sink.

3 Maximal global Lyapunov exponents

In order to further explore the effect on the dynamical evolution of the system of the emergence of the collective mode of expansion, we find useful to study the maximal Lyapunov exponent (MLE), which measures the rate of exploration of the available phase space. A convenient way to calculate the MLE is the following, we generate at time $t = 0$, for each trajectory, a second one where we change the momenta of the particles by a small amount d_0 in momentum space. Following [12], we define a distance between trajectories $d(t)$ as:

$$d(t) = \left(\frac{1}{N} \sum_{i=1}^{N} [a(\mathbf{r}_1(t) - \mathbf{r}_2(t))^2 + b(\mathbf{p}_1(t)) - \mathbf{p}_2(t))^2]_i \right)^{1/2},$$

where $\mathbf{r}, \mathbf{p}$ refer to the positions and momenta of N particles at time t. Indices 1 and 2 refer to the two trajectories differing by d_0 at $t = 0$. a, b are two arbitrary parameters which express the fact that the MLE are independent of the particular metrics in the phase space [22]. For the purpose of this paper, we will fix $a = 0, b = 1/m$ where m is the mass of the particles, *i.e.* distances in velocity space only. If we calculate numerically the time evolution of $d(t)$ solving the CEOM, we observe an exponential increase followed by saturation in velocity space [12,15,16]. The exponential increase of $d(t)$ is associated to the MLE $\hat{\lambda}$ and it implies the following relation: $\frac{{\rm d}d(t)}{{\rm d}t} = \hat{\lambda} d(t)$. But this rapid increase cannot last forever because the available velocity phase space is limited, giving rise to a saturation of the inter-trajectory distance in velocity space. In order to describe this saturation, we can consider the previous relation as a first-order term in an expansion in $d(t)$, going to second order we get [15]

$$\frac{{\rm d}d(t)}{{\rm d}t} = \hat{\lambda} d(t) - \alpha d^2(t) + .. \,,$$

where α is a constant greater than zero for fully developed chaos. This equation can be easily solved, giving:

$$d(t) = \frac{d_\infty d_0}{d_0 + (d_\infty - d_0) e^{-\hat{\lambda} t}}\,, \tag{4}$$

$$\hat{\lambda} = \alpha d_\infty\,, \tag{5}$$

where $d_0 = d(t = 0)$ and $d_\infty = d(t = \infty)$. Thus, eqs. (4),(5) tell us that, to characterize the entire time evolution of $d(t)$, we need three quantities, λ, the asymptotic distance between trajectories d_∞ and α, but only two quantities are independent because of eq. (5). In particular, if α is a constant, we find that the LE are proportional to d_∞. In ref. [15] this relation was supported from numerical simulation in Hamiltonian systems, similarly in ref. [16] for maps.

The MLE is proportional to the distance in velocity space which provides a measure of the fluctuations. For instance for an infinite system in equilibrium as $t \to \infty$, the momenta of particles in event 1 are uncorrelated to those of event 2, and it is very easy to show that in such

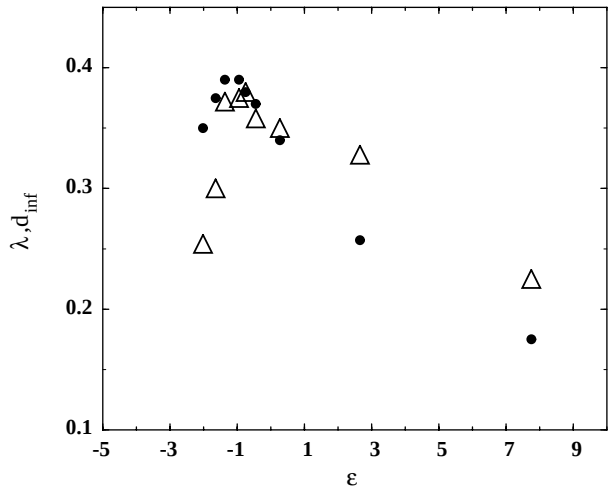

Fig. 2. MLE (triangles) and $d_\infty/4$ (full circles) as a function of energy for two-dimensional Lennard-Jones drops with $N = 100$ particles.

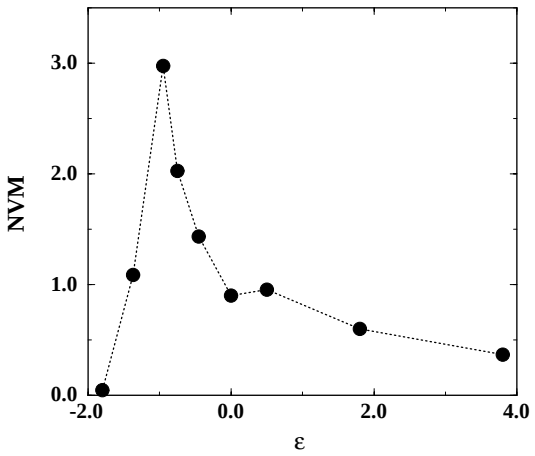

Fig. 3. Normalized Variance of the Maximum fragment (NVM) as a function of the energy of the fragmenting system.

cases the d_∞ is proportional to the variance in velocity space. This is a very useful result which allows us to estimate the LE using the final distributions obtained either from the data or from the theory such as the thermodynamics. For example, for a classical Boltzmann gas the variance of the velocity distribution σ is given by [1]

$$d_\infty \propto \sigma = \left(\frac{3T}{m}\right)^{1/2}, \tag{6}$$

where T is the temperature of the gas measured in units of energy. For the infinite system, the MLE is then an increasing function of the temperature of the system [15, 23]. On the other hand, in the case of a free expansion of a finite system (collective motion), $d_\infty = d_0$ holds, *i.e.* $\hat{\lambda} = 0$.

In fig. 2 we plot the MLE and the d_∞ *vs.* energy ϵ as obtained in our CMD simulations. The qualitative features are the same as those obtained in ref. [12,15]. Both quantities plotted display a maximum even though at slightly different ϵ. The decrease of the d_∞ for large ϵ, suggests that the particles having an initial kinetic energy larger than the binding energy escape quickly from the system without interacting. In fact, if we compare this figure with the caloric curve displayed in fig. 1 we will notice that d_∞ attains its maximum when the caloric curve reaches the plateau, which signals the state at which the dynamics of the system begins to be characterized by the presence of a collective radial flow.

The maximum in the MLE is shifted with respect to the one of the d_∞, in order to clarify the meaning of this maximum we show in fig. 3 the behavior of the Normalized Variance of the Maximum fragment defined as

$$\mathrm{NVM} = \frac{\langle A_{\max} - \langle A_{\max}\rangle\rangle^2}{\langle A_{\max}\rangle}, \tag{7}$$

where $A_{\max}$ stands for the size of the maximum fragment in each fragmentation event and $\langle ...\rangle$ denote the average over an ensemble of event at a given energy. This quantity has been discussed in [13,14] and it was shown that it displays a peak in the critical region. We then notice that both the MLE and NVM display a maximum for the same energy of the fragmenting system. So the MLE reaches a maximum for that energy for which the fluctations are maximal and where we expect to find critical behavior

When the evolution of the system is dominated by the ordered collective motion, the rate of exploration of phase space is reduced, *i.e.* the MLE decreases. This supports also the idea of a limiting temperature that a finite system can sustain [5,9,24].

The maximum in the MLE signals a transition from a chaotic to a more ordered motion, *i.e.* a motion in which the expansion collective mode becomes more and more important. For a finite system, the main effect of collective motion is to suppress inter-particle collisions, in fact the higher the initial energy, the faster the systems breaks and the smaller the final fragments are. Such a behavior resembles the one that has already been observed in [25] in a liquid to solid transition for the correlated cell model when changing the density. Notice indeed the similarity of the two cases. Small ϵ in our case corresponds to small ρ in [25], *i.e.* the chaotic motion occurs in the liquid. At high ϵ, we obtain a more ordered motion because of the collective expansion, while in [25] at high ρ the system becomes a solid displaying regular trajectories which remains trapped within the volume determined by the neighboring particles.

4 Generalized entropies and fractal dimensions

If our simulations are followed for a long time, stable fragments will finally be formed. From the mass distributions, we can estimate the GRE as follows. Define the probability of finding a fragment of mass i as the number of fragments $M(i,\delta)$, where δ is the mass resolution, divided the total number of fragments produced for a given event

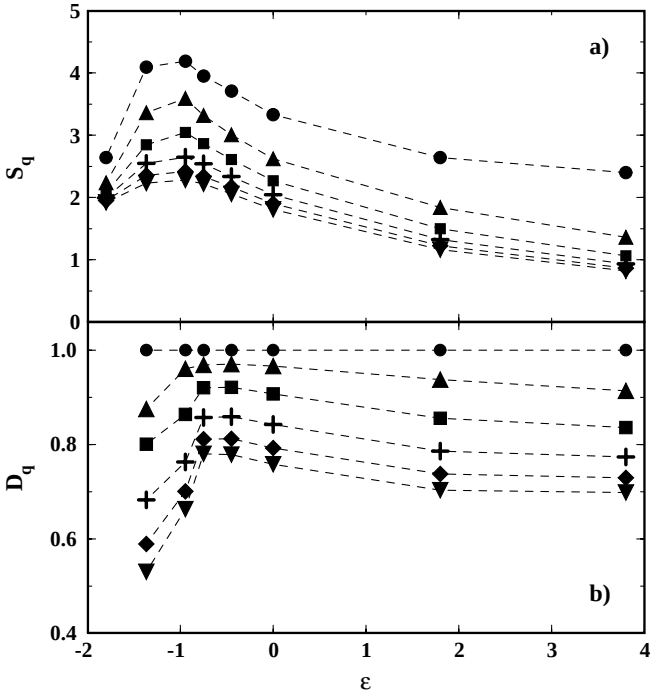

Fig. 4. a) Generalized entropies and b) fractal dimensions *vs.* energy calculated from the asymptotic mass spectra for the same system as fig. 1. Full circles $q = 0$, full triangles $q = 1$, full squares $q = 2$, crosses $q = 3$, full diamonds $q = 4$, down pointing triangles $q = 5$.

at that ϵ. Thus,

$$p(i,\delta) = \frac{M(i,\delta)}{\sum M(i,\delta)} \,. \tag{8}$$

GRE are defined as [17]

$$S_q(\delta) = \frac{1}{1-q} \log \left(\sum_i \langle p_i \rangle^q \right) \,,$$

where $\langle\,\rangle$ denote the average over an ensemble and we take q as an integer number. It is important to stress that the minimum mass resolution possible for finite systems is clearly $\delta = 1$.

In fig. 4a) we plot $S_q(\delta = 1)$ *vs.* ϵ, for $q = 0$–5 a clear peak is observed. This peak is precisely in the region in which the MLE also shows a peak. Note that in the calculations we restricted the sum to those particles having mass larger than 2. If we keep smaller masses, the peak remains even though it broadens.

From the knowledge of the GRE we can define the Generalized Dimensions (GD) as:

$$D_q = \frac{\lim}{\delta \to 0} \frac{S_q(\delta)}{\log \delta} \,,$$

i.e. we study the way in which $S_q(\delta)$ scales with δ [26]. In fig. 4b) we show the fractal dimension D_q *vs.* ϵ. It is once again immediate to see a peak in D_q ($q \geq 1$) in the same region in which MLE and S_q displayed a peak. Finally, in fig. 5 we plot the D_q *vs.* q for various excitation energies.

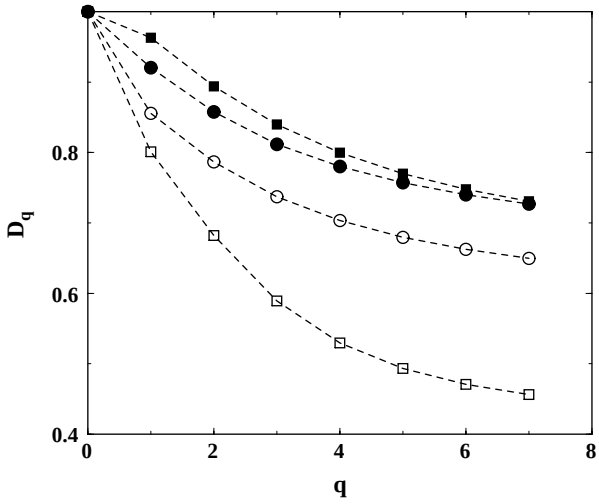

Fig. 5. Generalized fractal dimensions at $\epsilon = -1.37$ (open circles) -0.75 (full circles) and 2.25 (open squares). The full squares are obtained assuming a power law mass distribution.

By way of illustration we discuss some limiting cases. For instance, if the mass distribution is uniform, we easily get $D_q = 1$ for all q. This is a trivial case which tells us that the entire space is uniformly covered and the D_q are equal to the topological dimension 1. Another limiting case is when all the particles are concentrated in one bin (say mass 1) and zero otherwise. This gives $D_q = 0$ which is the dimension of the space occupied, *i.e.* the dimension of a point. It is also interesting to note that if the p_i's are different from 0 for M contiguous bins only, then $D_0 = 1$, *i.e.* the Hausdorff dimension of a segment. A more interesting case is when the mass distribution is given by a power law. We can write such a mass distribution as $y(x) \propto x^{-\tau}$, where $x\epsilon[\epsilon, 1]$, $x = i/N$ and ϵ is a small quantity related to the smallest possible mass that we can have. Following [17], taking the limits $\delta \to \epsilon \to 0$ gives, for $\tau < 1$:

$$D_q = \begin{cases} 1; & q < 1/\tau; \\ q(1-\tau)/(q-1); & q \geq 1/\tau \,. \end{cases}$$

For instance, $\tau = 0.5$ gives the GD as for the logistic map at $r = 4$ [17] with D_q continuous, but its first derivative has a discontinuity at $q = 2$ and this behavior is referred to as a first-order phase transition. As we noticed before, in our case we get a power-law distribution for the excitation energy where the MLE and the GRE have a maximum. Since the power that we get is larger than 2, it is interesting to see what the behavior of the D_q is in such a case, which corresponds to a second-order phase transition (at least in the infinite case limit). First, we have simulated numerically a power-law yield and the result is plotted in fig. 5 (full squares), for a system composed of 100 particles and $\tau = 2.1$. The CMD results for $\epsilon = -0.75$ (full circles) where a power law in the mass distribution is obtained, are in good agreement with the

simulation. We notice that the D_q show no discontinuities at variance with the cases where $\tau \leq 1$. In order to test if this is a finite size effect, we have simulated fragmentation in a simple percolation model whose properties are well studied. We find a similar behavior for the one discussed above at the critical percolation point and for very large sizes more details will be discussed elsewhere. The D_q are also plotted for the cases when d_∞ has a maximum (open circles) and at high ϵ (open squares). The functional dependence of D_q on q suggests a multifractal character of the probability distributions.

5 Conclusions

From these analysis the behavior of excited finite systems is greatly clarified. If we start with a cold (solid) drop of matter and begin to heat it up the Lyapunov exponent increases as well as the d_∞. The first one is proportional to the rate at which the system explores phase space and the second to the available phase space. This trend changes as the rate of evaporation increases, *i.e.* when radial flow, the extra degree-of-freedom characteristic of the evolution of highly excited finite systems, starts to play a major role in the evolution. A maximum of both quantities is reached when the system approaches the critical region, *i.e.* when fluctuations are maximal and the final spectra contain both liquid-like and vapor-like components. For even higher excitation energies both magnitudes decrease as a result of the fast fragmentation process and the transfer of chaotic (thermal) energy into ordered (radial flux) energy. A peak is also observed in the generalized Renyi entropies and in the generalized fractal dimensions D_q. The D_q at the "critical" point for which a power law with $\tau \geq 2$ is obtained is a smooth decreasing function of q at variance with the cases where $\tau \leq 1$.

References

1. L. Landau, E. Lifshits, *Statistical Physics* (Pergamon, New York, 1980); K. Huang, *Statistical Mechanics*, second edition (J. Wiley, New York, 1987).
2. S.K. Nayak, R. Ramaswamy, C. Chakravarty, Phys. Rev. E **51**, 3376 (1995).
3. P. Labastie, W. Wheten, Phys. Rev. Lett. **65**, 1567 (1990).
4. M. Schmidt *et al.*, Phys. Rev. Lett. **86**, 1191 (2001).
5. A. Bonasera, Phys. World **12**, 20 (1999); V. Latora, M. Belkacem, A. Bonasera, Phys. Rev. Lett. **73**, 1765 (1994); P. Finocchiaro, M. Belkacem, T. Kubo, V. Latora, A. Bonasera, Nucl. Phys. A **600**, 236 (1996).
6. A. Bonasera, M. Bruno, C.O. Dorso, P.F. Mastinu, Riv. Nuovo Cimento n. 2, **23** (2000).
7. M.L. Gilkes *et al.*, Phys. Rev. Lett. **73**, 1590 (1994); P.F. Mastinu *et al.*, Phys. Rev. Lett. **76**, 2646 (1996); M. D'Agostino *et al.*, Nucl. Phys. A **650**, 329 (1999).
8. B. Farizon *et al.*, Phys. Rev. Lett. **81**, 4108 (1998).
9. A. Strachan, C.O. Dorso, Phys. Rev. C **52**, R632 (1998); A. Strachan, C.O. Dorso, Phys. Rev. C **59**, 285 (1999).
10. M. D'Agostino *et al.*, Phys. Lett. B **473**, 219 (1999).
11. A. Chernomoreta, M. Ison, S. Ortiz, C.O. Dorso, Phys. Rev. C **64**, 024606 (2001); arXiv:nucl-th/0101061.
12. A. Bonasera, V. Latora, A. Rapisarda, Phys. Rev. Lett. **75**, 3434 (1995).
13. C.O. Dorso, V. Latora, A. Bonasera, Phys. Rev. C **60**, 034606 (1999).
14. X. Campi, J. Phys. A **19**, 917 (1986); Phys. Lett. B **208**, 351 (1988).
15. A. Bonasera, V. Latora, M. Ploszaijck, Ganil preprint, june 1996, unpublished.
16. V. Baran, A. Bonasera, chao-dyn/9804023.
17. B. Mandelbrot, *The Fractal Geometry of Nature* (W. Freeman & Co., San Francisco, 1983); J.L. McCauley, *Chaos Dynamics and Fractals, Cambridge Nonlinear Science Series 2* (Cambridge University Press, 1993); E. Ott, *Chaos In Dynamical Systems* (Cambridge University Press, 1993); R.C. Hilborn, *Chaos and Nonlinear Dynamics* (Oxford University Press, New York, 1994); M. Schroeder, *Fractals, Chaos, Power Laws* (W. Freeman & Co., 1991); H.G. Schuster, *Deterministic Chaos* (VCH editions, 1995).
18. D. Frenkel, B. Smit, *Understanding Molecular Simulations* (Academic Press, San Diego, London, 1996).
19. C.O. Dorso, J. Randrup, Phys. Lett. B **301**, 328 (1993).
20. C.O. Dorso, J. Aichelin, Phys. Lett. B **345**, 197 (1995); T. Reposeur, F. Sebille, V. De La Mota, C.O. Dorso, Z. Phys. A **357**, 79 (1997).
21. C.O. Dorso, A. Strachan, Phys. Rev. B **54**, 236 (1996); A. Strachan, C.O. Dorso, Phys. Rev. C **35**, 775 (1997).
22. We remark that if the collective effects are important, then the calculations of the MLE become sensitive to the time when the second trajectory is generated. Here, we are always referring to the MLE as obtained by generating a second trajectory at $t = 0$ [12].
23. I. Borzsak, A. Baranyai, H. Posch, Physica A **229**, 93 (1996).
24. R. Wada *et al.*, Phys. Rev. C **39**,497 (1988).
25. C. Dellago, H.A. Posch, Physica A **230**, 364 (1996); C. Dellago, H.A. Posch, W.G. Hoover, Phys. Rev. E **53**, 1485 (1996).
26. Notice that even though the minimum possible mass is $\delta = 1$, when plotting $S_q(\delta)$ *vs.* δ in log-log scale we can extrapolate to $\delta \to 0$. We would like to stress that the range where the fit is performed , see eq. (8) and following, is limited due to the finiteness of the system.